This article has been accepted for publication in IEEE Communications Letters. This is the author's version which has not been fully edited and content may change prior to final publication. Citation information: DOI 10.1109/LCOMM.2024.3376713

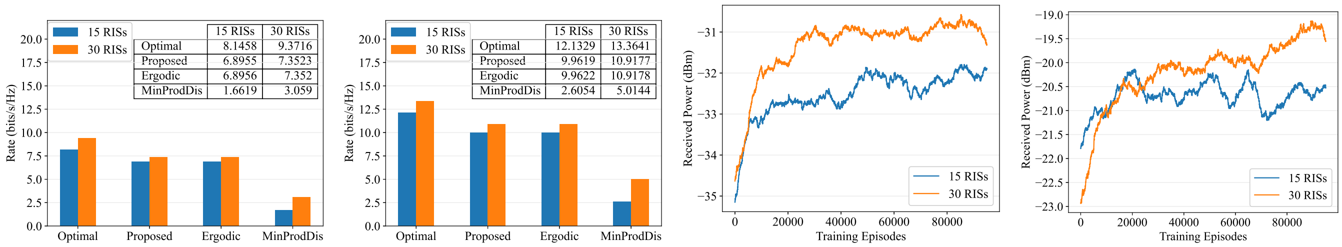

(a) 100 × 100 elements (b) 200 × 200 elements (c) 100 × 100 elements (d) 200 × 200 elements

Fig. 2: Comparison on the achievable rates and the training curves of the proposed approach.

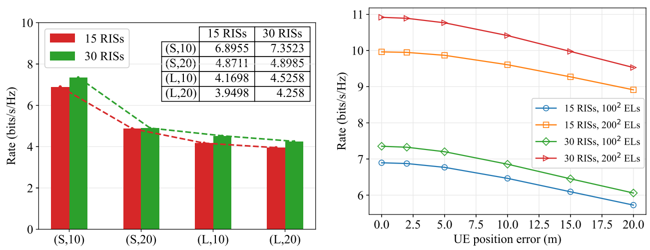

(a) Different blockage cases. (b) Different UE position errors.

Fig. 3: The impact of different blockage cases and UE position errors on the performance of the proposed approach.

sizes (small (S) and large (L)). Fig. 3a shows the achievable rates in scenarios where 15 and 30 RISs, both equipped with 100×100 elements, are deployed. We can see that even severe blockages have very limited impact ($\leq$ 3 bits/s/Hz rate decrease) on the performance of the *Proposed*. When the number or size of obstacles is small, increasing the other factor considerably cuts down the rates, whereas when either factor is large, the impact of increasing the other is quite limited.

Then, we test the *Optimal* and *Proposed* on different UE speed ranges ($[2, 20]$ m/s and $[20, 60]$ m/s) in scenarios with 10 small obstacles. The achievable UE rates are listed in Table I. As expected, both approaches see slight rate decreases as UE speeds are increased. Despite the number of RIS elements, both approaches exhibit about 0.015 and 0.005 bits/s/Hz rate decrease for 15 and 30 RISs, respectively. 30 RISs enable less rate decrease, because more RISs can serve more UE positions.

Finally, we test the sensitivity of the *Proposed* to the UE position estimation errors (from 0 m to 20 m), in the scenarios with 10 small obstacles. As can be seen from Fig. 3b, despite the RIS settings, as the UE position error increases, the UE rates decrease at a close rate. The rate decrease is not evident when the UE position error is less than 5 m. The rate decreases corresponding to 10 m and 20m are 0.5 and 1 bits/z/Hz. This demonstrates that the *Proposed* is not sensitive to the UE position error, therefore, can be used to achieve satisfactory rates even with outdated UE position information due to time costs of positioning and RIS configuration procedures.

V. Conclusion

In this letter, we have investigated a real-time RIS switch approach for mobile mmWave network scenarios where multiple RISs are installed and the associated redirected propagation paths could be blocked by obstacles. We have resorted to the actor-critic technique to learn uncertain obstacles and constantly changing spatial conditions caused by the mobile user. Finally, we have derived the ergodic rate achievable with the proposed approach. The experimental results carried out in different scenarios have shown that the proposed RIS switch approach can effectively learn unknown environmental features and approximate the optimal strategy. It can even approach the ideal optimum with only around 15% gap and outperform the state-of-the-art by 76%.

References

[1] S. Zeng, H. Zhang, B. Di, Z. Han, and L. Song, "Reconfigurable intelligent surface (ris) assisted wireless coverage extension: Ris orientation and location optimization," *IEEE Commun. Lett.*, vol. 25, no. 1, pp. 269–273, 2020.
[2] Z. Lian *et al.*, "A novel geometry-based 3-d wideband channel model and capacity analysis for irs-assisted uav communication systems," *IEEE Trans. Wireless Commun.*, 2023.
[3] J. Xu *et al.*, "Reconfiguring wireless environments via intelligent surfaces for 6g: Reflection, modulation, and security," *Science China Information Sciences*, vol. 66, 2023.
[4] M. He, J. Xu, W. Xu, H. Shen, N. Wang, and C. Zhao, "Ris-assisted quasi-static broad coverage for wideband mmwave massive mimo systems," *IEEE Trans. Wireless Commun.*, vol. 22, no. 4, pp. 2551–2565, 2023.
[5] K. Feng, Q. Wang, X. Li, and C. K. Wen, "Deep reinforcement learning based intelligent reflecting surface optimization for miso communication systems," *IEEE Wireless Commun. Lett.*, no. 99, 2020.
[6] N. Mensi and D. B. Rawat, "Reconfigurable intelligent surface selection for wireless vehicular communications," *IEEE Wireless Commun. Lett.*, vol. 11, no. 8, pp. 1743–1747, 2022.
[7] Y. Fang, S. Atapattu, H. Inaltekin, and J. Evans, "Optimum reconfigurable intelligent surface selection for wireless networks," *IEEE Trans. Commun.*, vol. 70, no. 9, pp. 6241–6258, 2022.
[8] C. Huang, R. Mo, and C. Yuen, "Reconfigurable intelligent surface assisted multiuser miso systems exploiting deep reinforcement learning," *IEEE J. Sel. Areas Commun.*, vol. 38, no. 8, pp. 1839–1850, 2020.
[9] Q. Zhang, W. Saad, and M. Bennis, "Millimeter wave communications with an intelligent reflector: Performance optimization and distributional reinforcement learning," *IEEE Trans. Wireless Commun.*, vol. 21, no. 3, pp. 1836–1850, 2021.
[10] W. Tang *et al.*, "Path loss modeling and measurements for reconfigurable intelligent surfaces in the millimeter-wave frequency band," *IEEE Trans. Commun.*, vol. 70, no. 9, pp. 6259–6276, 2022.
[11] 3GPP, *Study on channel model for frequencies from 0.5 to 100 GHz, TR 38.901*.
[12] V. Mnih *et al.*, "Asynchronous methods for deep reinforcement learning," in *ICML*, 2016, pp. 1928–1937.
[13] Y. F. Wu, W. ZHANG, P. Xu, and Q. Gu, "A finite-time analysis of two time-scale actor-critic methods," in *NIPS*, 2020, pp. 17 617–17 628.
[14] R. Livni, S. Shalev-Shwartz, and O. Shamir, "On the computational efficiency of training neural networks," in *NIPS*, 2014, pp. 855–863.